

Supporting information

Hybrid assemblies of a symmetric designer protein and polyoxometalates with matching symmetry

Laurens Vandebroek^{b,c,†}, Hiroki Noguchi^{a,†}, Kenichi Kamata^d, Jeremy R.H. Tame^d, Luc Van Meervelt^c, Tatjana N. Parac-Vogt^b and Arnout R.D. Voet^{*a}

*a. Laboratory for biomolecular modelling and design, KU Leuven Department of Chemistry, Celestijnenlaan 200G, 3001 Leuven, Belgium.
E-mail: arnout.voet@kuleuven.be*

b. Laboratory for bioinorganic chemistry, KU Leuven Department of Chemistry, Celestijnenlaan 200F, 3001 Leuven, Belgium.

c. Biomolecular architecture, KU Leuven Department of Chemistry, Celestijnenlaan 200F, 3001 Leuven, Belgium.

d. Drug Design Laboratory, Yokohama City University 1-7-29, Suehiro, Tsurumi, Yokohama, 230-0045 (Japan)

† These authors contributed equally.

Abstract: Novel bioinorganic hybrid materials based on proteins and inorganic clusters have enormous potential for the development of hybrid catalysts that synergistically combine properties of both materials. Here we report the creation of hybrid assemblies between a computationally designed symmetrical protein Pizza6-S and different polyoxometalates with matching symmetry: the tellurotungstic Anderson-Evans ($\text{Na}_6[\text{TeW}_6\text{O}_{24}] \cdot 22\text{H}_2\text{O}$) (TEW); Keggin ($\text{H}_4[\text{SiW}_{12}\text{O}_{40}] \cdot 6\text{H}_2\text{O}$) (STA); and 1:2 Ce^{III}-substituted Keggin ($\text{K}_{11}[\text{Ce}^{\text{III}}[\text{PW}_{11}\text{O}_{39}]_2] \cdot 20\text{H}_2\text{O}$) (Ce-K). This results in the formation of complexes with clearly defined stoichiometries in solution. Crystal structures validate the complexes as building blocks for the formation of larger assemblies.

Table of Contents

Table of Contents	2
Experimental Procedures	3
Results and Discussion	5
Figure S1. Determination of binding affinity by fluorescence quenching and ITC.	5
Figure S2. Sedimentation coefficient distribution of Pizza6-S:POM complexes at different pH. The 50 μ M POM solution (dashed line), 38.9 μ M Pizza6-S (blue line), 0.19 molar ratio (POM/Pizza6-S, green line), 0.47 molar ratio (yellow line) and 0.98 molar ratio (red line).	6
Figure S3. Images of crystals. Typical crystals are shown used in the determination of each structure described.	7
Figure S4. Anomalous diffraction maps confirming W and Ce atom positions.	8
Figure S5. The interaction distances of POMs with Pizza6-S observed in the crystallographic models for (a) STA (space group C2) and (b) Ce-K.	9
Figure S6. Contacts between STA and the neighbouring Pizza6-S are mediated by hydrogen bonds to histidine residues only (C2). The hydrogen bonds between STA and the interacting residues shown as a dashed line (a). An overall view of the hybrid assembly as observed in the crystal structure (b). Measured distances for the observed interactions (c).	10
Figure S7. The position of the clathrate STA in the C2 crystal structure, away from the symmetry axis of the protein (C2).	10
Figure S8. Comparison of STA and Ce-K binding to the face of Pizza6-S in unbuffered conditions.	11
Figure S9. Alternate orientations of the POMs in the Pizza6 + TEW (a) and Pizza6 + STA ($P2_1$) (b) crystals.	12
Figure S10. The Keggin and Anderson-Evans type POMs binding mode is not influenced by crystal packing contacts in the crystallisation buffer at pH 6 or above.	13
Figure S11. Complementarity and shape and hydrogen bonding determines specificity of the Pizza6S for Keggin type over Anderson-Evans type POMs.	14
Figure S12. Comparison of STA binding under buffered conditions with STA and Ce-K under unbuffered conditions.	15
Table S1. The effect of NaCl on binding affinity of Pizza6-S and POM at pH 6.	16
Table S2. Overview of crystallisation conditions.	16
Table S3. Crystallographic data collection and refinement statistics.	17
Table S4. The occupancies of TEW, STA and Ce-K in their respective co-crystals.	18
Table S5. Calculated volume and percentage of voids in the crystal packings.	19
References	20
Author Contributions	21

Experimental Procedures

Expression and purification of Pizza6-S protein

A synthetic linear DNA fragment encoding Pizza6-S(1) was purchased from IDT (Belgium), and cloned into pET28b vector (Novagen) using the NdeI and XhoI restriction sites. The protein was expressed and purified as previously described.(2) The purified protein was concentrated to 10-20 mg/mL using a Vivaspin15R (Sartorius), and purity was estimated to be at least 95% by SDS-PAGE.

Synthesis of polyoxometalates (POMs)

Silicotungstic acid hydrate, $H_4[SiW_{12}O_{40}] \cdot 6H_2O$ (STA), was purchased from Sigma-Aldrich in the highest available purity grade and used without further purification. The compound was dried in a drying oven for several hours to obtain the hexahydrate from the n-hydrate for improved accuracy in subsequent experiments.(3)

The tellurotungstate Anderson-Evans, $Na_6[TeW_6O_{24}] \cdot 22H_2O$ (TEW), was synthesized according to a published protocol.(4) A solution of 5.00 g of $Na_2WO_4 \cdot 2H_2O$ and 0.60 g $Te(OH)_6$ in 100 mL H_2O was adjusted to pH 5.0 using 1 M HCl. The solution was then heated to 100°C and evaporated until the volume was reduced by 25%. After cooling, the solution was filtered and left to crystallize at room temperature. Colorless crystals of $Na_6[TeW_6O_{24}] \cdot 22H_2O$ were obtained after several days. The crystals were filtered, air dried and then characterized using IR spectroscopy.

The 1:2 Ce^{III} -Phosphotungstic Keggin, $K_{11}[Ce^{III}[PW_{11}O_{39}]_2] \cdot 20H_2O$ (Ce-K), was synthesized using the method of Griffith *et al.*(5) $H_3[PW_{12}O_{40}] \cdot nH_2O$ was dissolved in 5 mL hot H_2O . Directly after dissolving, a fresh solution of 0.75 mmol $Ce(NO_3)_3 \cdot 6H_2O$ in 2 mL H_2O was added, followed by 5.0 g potassium acetate in 5 mL H_2O . The pH of the solution was adjusted to 7 by the dropwise addition of acetic acid with vigorous stirring. The solution was filtered and stored in the refrigerator for crystallization. After 1-2 days, the brown-orange crystals were collected by filtration and air-dried. The compound was characterized using ^{31}P NMR.

Tryptophan fluorescence

Tryptophan fluorescence was used as a fast primary screen to identify binding by deriving K_d values. Experiments were performed in 96-well microplates (Greiner) on a Safire2 (TECAN). The Pizza6-S protein was diluted to 6.09 μM in 20 mM sodium acetate pH 5, MES pH 6, MOPS pH 7, HEPES pH 8 and Bicine pH 9. The tryptophan quenching by different concentrations of POM were recorded at 300-400 nm (emission wavelength) and 280 nm excitation. The data analysis was done by least-squares fitting of the data to a derived Stern-Volmer equation using emission at 330 nm wavelength.(6)

Isothermal titration calorimetry

ITC experiments were carried out with a MicroCal VP-ITC (Malvern). Purified Pizza6-S protein was placed in the cell and maintained at a temperature of 298.15 K. The POM solutions were dissolved in the same buffer as the protein and were injected to the cell. Buffers at different pH values were used with zero or 100 mM NaCl: 50mM sodium acetate pH 5, MES pH 6, MOPS pH 7, HEPES pH 8, and Bicine pH 9. 28 injections of the ligand solution, 10 μL each, were made in total, allowing the baseline to stabilise between injections. The raw data were analysed using NITPIC(7-9), SEDPHAT(8,10) software with single binding site model. The figures were made with GUSI.(11)

Analytical Ultracentrifugation

Sedimentation velocity experiments were carried out using an Optima XL-I analytical ultracentrifuge (Beckman-Coulter, Fullerton, CA) using an An-50 Ti rotor. For sedimentation velocity experiments, cells with a standard Epon two channel centrepiece and sapphire windows were used. 400 μL of protein (38.9 μM) or 400 μL mixture solution with POMs (10, 25 and 100 μM) and 420 μL of reference buffer were used in each experiment. The same pH buffers were used as with the ITC measurement, with the addition of 100 mM NaCl in each experiment. The rotor temperature was equilibrated at 20°C in the vacuum chamber for 1.5 hours prior to starting each measurement. Absorbance (280 nm) and interference scans were collected at 10 min. intervals during sedimentation at 50,000 rpm. The resulting scans were analysed using the continuous distribution c(s) analysis module in the program SEDFIT.(12) The partial specific volume of the proteins, solvent density, and solvent viscosity were calculated using the program SEDNTERP.(13)

Crystallization, structure determination and refinement

20 mg/mL Pizza6-S protein in 20 mM HEPES pH 8.0 was subjected to crystal screening in sitting-drop 96-well plates using sparse matrix kits (Qiagen) at 20°C. 0.25 μL drops of protein were mixed with 0.25 μL of 3.5 mM POMs solution (TEW, STA, 1:2 Ce-K) in water. 0.3 μL drops of 10 mg/mL Pizza6-S were used for apo-protein crystallization. All crystallization reservoir solutions are described in Supplementary Table A6.1. All crystals were cryo-cooled using 20-30% glycerol as cryo-protectant. X-ray diffraction data were collected on beamline

I-04 of the Diamond Light Source (Oxfordshire, UK) and beamline Proxima-1 of the SOLEIL synchrotron (Gif-sur-Yvette, France) using a PILATUS 6M-F detector (Dectris). Diffraction images were processed with XDS(14,15) and scaling was performed with AIMLESS(16). Molecular replacement performed using PHASER(17) with the Pizza structure (PDB: 3WW9)(2) as a template gave suitable solutions. Refinement was performed with PHENIX.REFINE(18,19) and COOT(20). The completed structures were validated with MolProbity.(21) Data collection and refinement statistics are given in Supplementary Table 2. The coordinates and structure factor data have been deposited with the Protein Data Bank with entry codes: 6QSD (Pizza6-S), 6QSE (Pizza6S-TEW), 6QSF (Pizza6-S with STA), 6QSG (Hybrid bioinorganic complex with Pizza6-S and STA), and 6QSH (Hybrid bioinorganic complex with Pizza6-S and Ce-K). Figures were generated in PyMOL.(22) Secondary structures were assigned with DSSP(23) and electronic potentials were calculated using APBS-PDB2PQR(24,25). Void volumes and percentages in the crystal packing were calculated using Mercury CSD 4.1.3 (Build 249162), using a probe of 1.2 Å and the solvent accessible surface.(26)

Generating the POM restraints

The restraints files, in CIF format, necessary for crystallographic refinement of the POMs were generated by two methods, depending on the structure of the POM. The tellurotungstate Anderson-Evans POM is available from the PDB under ligand code TEW and was imported directly into the model. The necessary restraints could be generated using the eLBOW(27) pipeline from the Phenix software suite and were edited, if necessary, with REEL.

Ligand models of silicotungstic acid(28) and Ce-K(29) had to be derived from their respective crystal structures as found on the Cambridge Structural Database, since they were not yet available on the PDB, and were manually fitted into the electron density using COOT(20). After merging these coordinates into a single PDB file, Refmac5(30) of the CCP4 software suite was used to generate suitable restraints automatically. These restraints were manually checked and corrected using REEL, until a final set of restraints was obtained that could be used for refinement. In order to permit rotational freedom around the Ce^{III}-ion, the bond angles and chiral volumes involving Ce were removed from the restraints library.

Results and Discussion

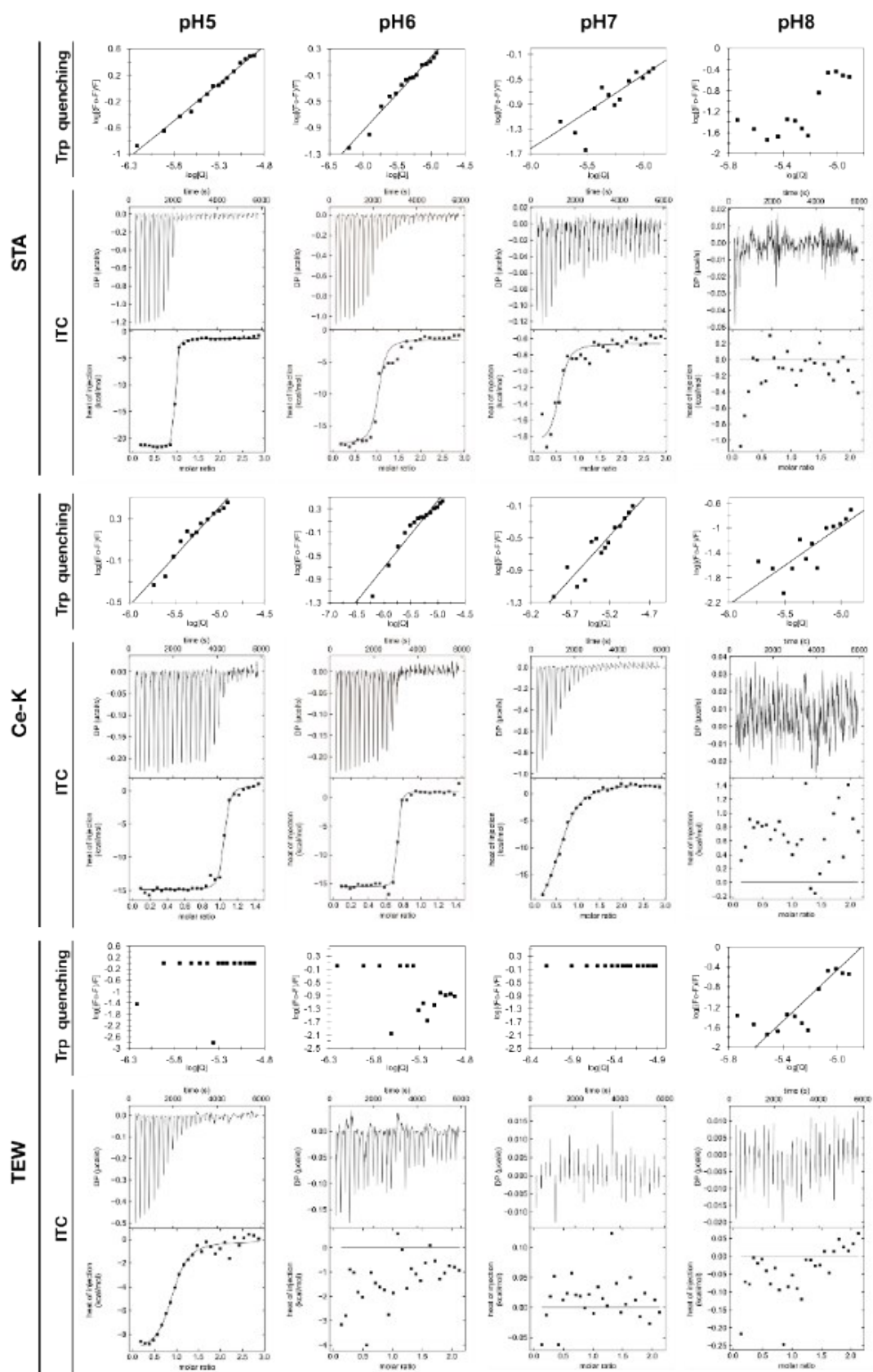


Figure S1. Determination of binding affinity by fluorescence quenching and ITC.

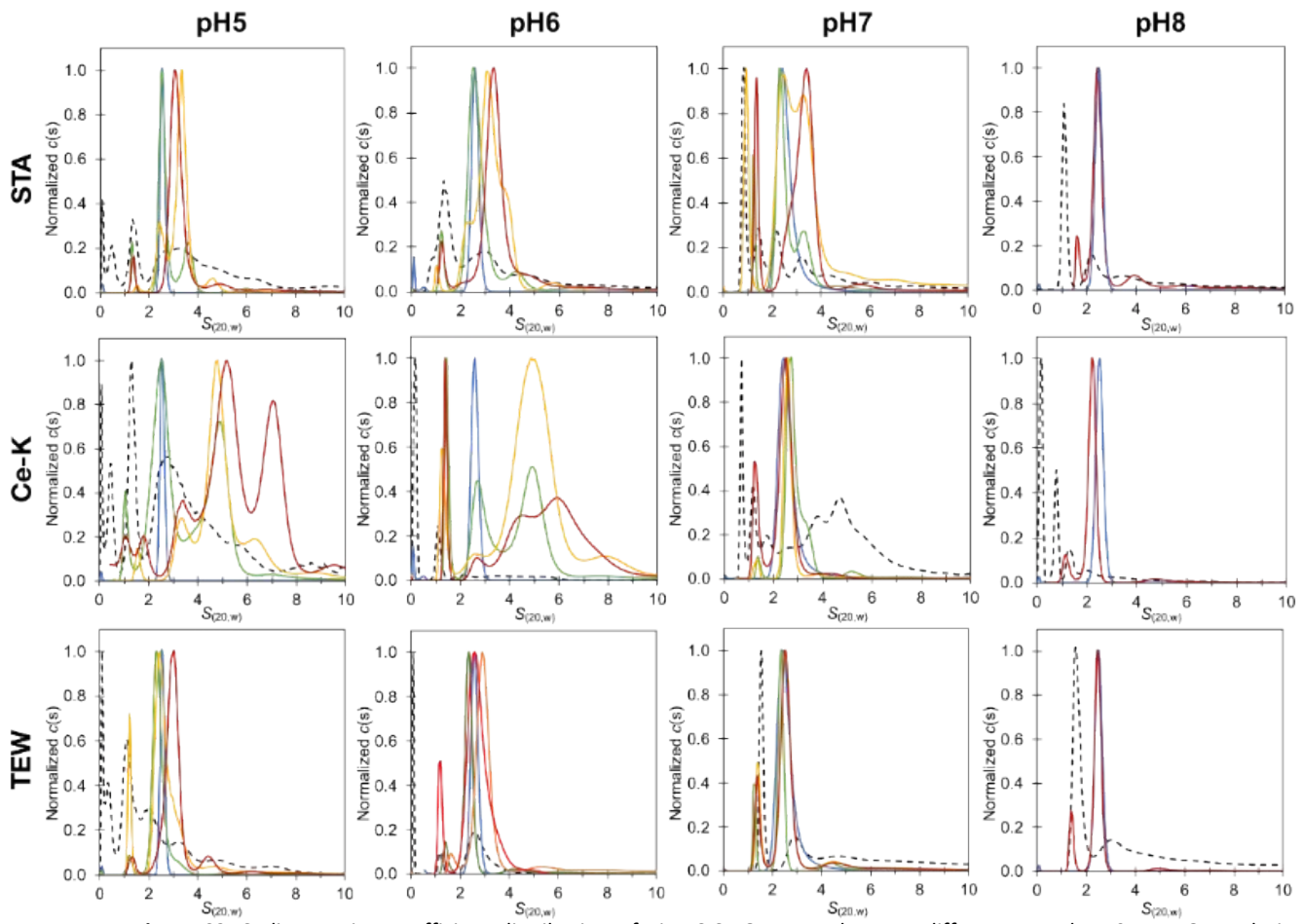
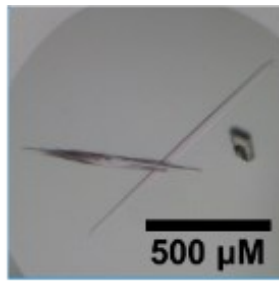
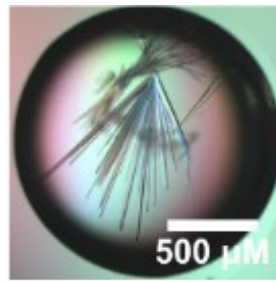


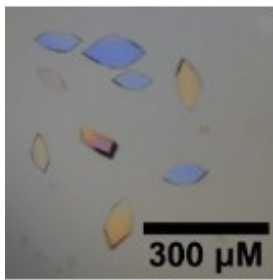
Figure S2. Sedimentation coefficient distribution of Pizza6-S:POM complexes at different pH. The 50 μM POM solution (dashed line), 38.9 μM Pizza6-S (blue line), 0.19 molar ratio (POM/Pizza6-S, green line), 0.47 molar ratio (yellow line) and 0.98 molar ratio (red line).



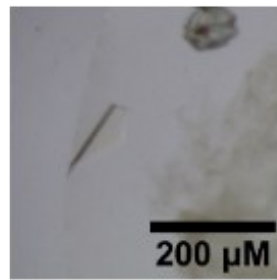
Apo state of Pizza6-S



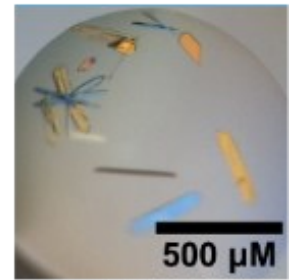
Pizza6-S with TEW



Pizza6-S with STA No.1



Pizza6-S with STA No.2



Pizza6-S with Ce-K

Figure S3. Images of crystals. Typical crystals are shown used in the determination of each structure described.

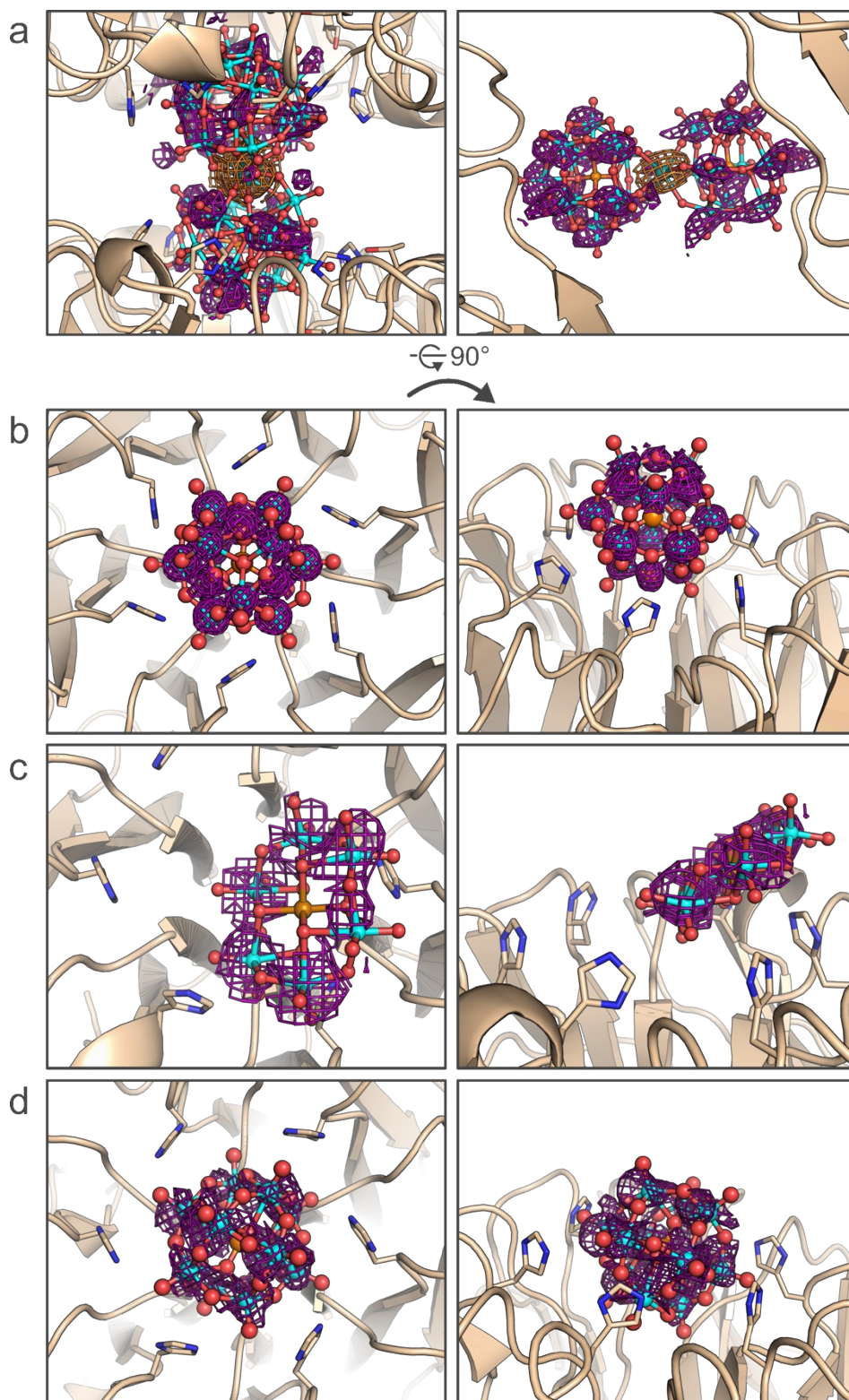


Figure S4. Anomalous diffraction maps confirming W and Ce atom positions.

Separate maps were calculated using anomalous differences observed using X-rays with wavelengths of 0.9795 Å and 1.85 Å, which are close to the L_1 edge of tungsten and cerium respectively. The map showing anomalous diffraction by W is coloured purple, and the map for Ce is shown in yellow, both maps being contoured at 2σ . (a) The Ce-K is shown bound to the faces of two Pizza6-S molecules (a, left) and between the sides of two protein molecules (a, right). (b) STA under acid conditions. (c) TEW under alkaline conditions. (d) STA under alkaline conditions, showing asymmetric interactions with the face of the protein.

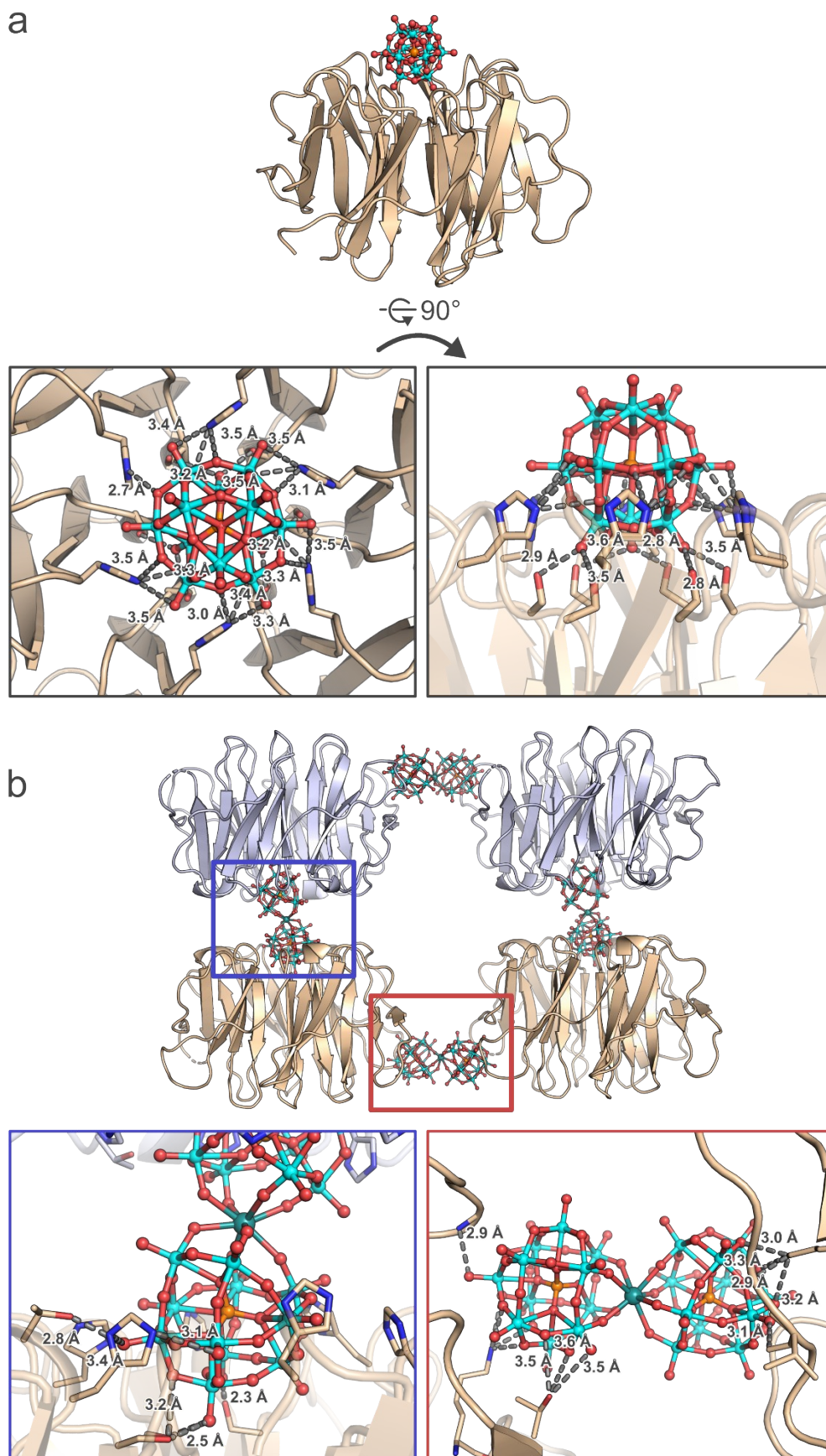


Figure S5. The interaction distances of POMs with Pizaa6-S observed in the crystallographic models for (a) STA (space group C2) and (b) Ce-K.

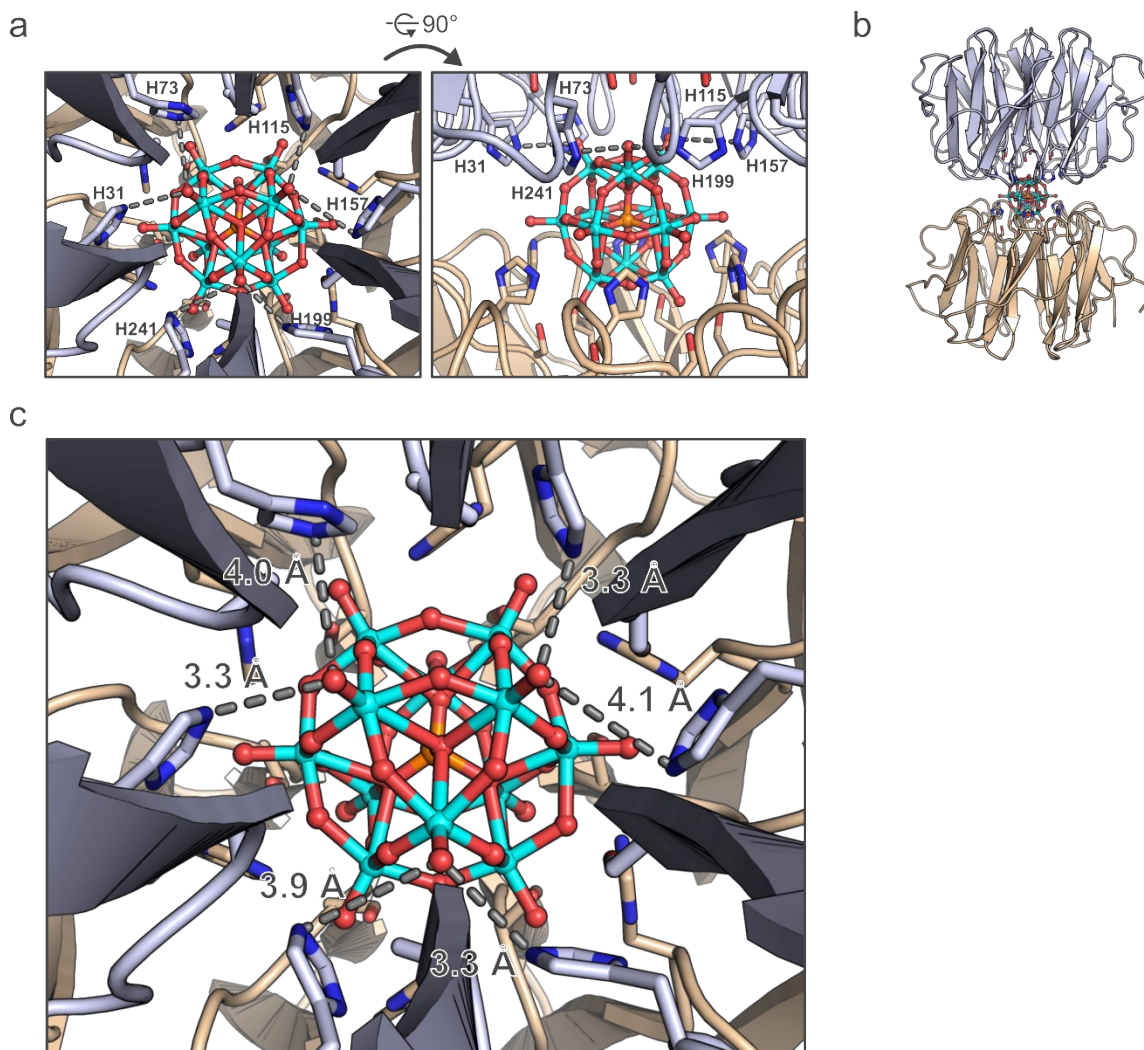


Figure S6. Contacts between STA and the neighbouring Pizaa6-S are mediated by hydrogen bonds to histidine residues only (C2). The hydrogen bonds between STA and the interacting residues shown as a dashed line (a). An overall view of the hybrid assembly as observed in the crystal structure (b). Measured distances for the observed interactions (c).

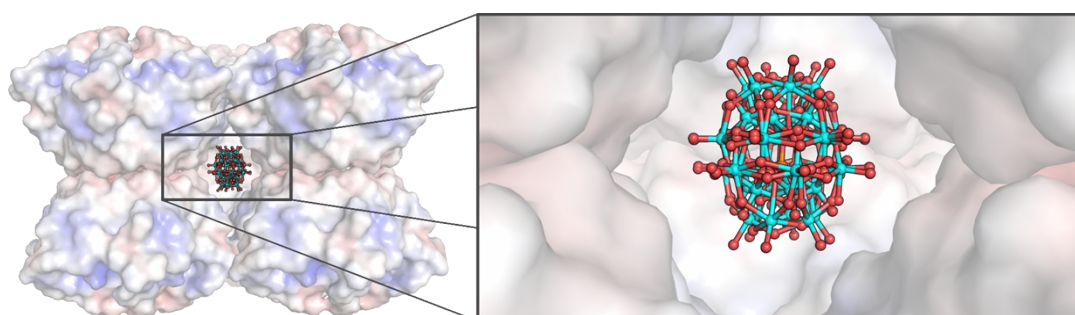


Figure S7. The position of the clathrate STA in the C2 crystal structure, away from the symmetry axis of the protein (C2).

The environment is largely apolar, with few direct interactions forming between the POM and protein. The sidechain of lysine 164 approaches the POM however, and stabilizes it within the cavity between protein molecules in the crystal.

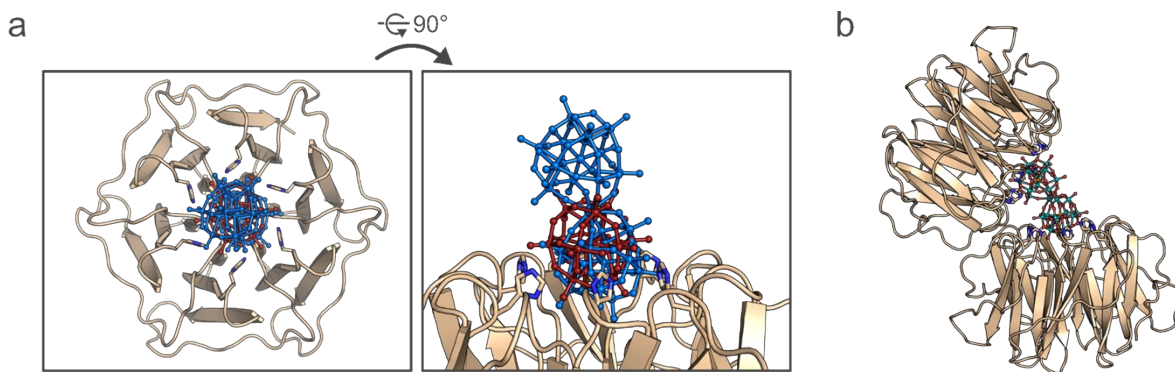


Figure S8. Comparison of STA and Ce-K binding to the face of Pizza6-S in unbuffered conditions.

The superposition of bound STA (C2, red) and Ce-K (blue) is shown in (a). Superposition of the Pizza6-S protein units on the Ce-K guided by the binding mode of individual Keggin units as observed in the STA binding mode in C2 reveals a highly distorted binding of the two Pizza6-S proteins resulting in a steric clash (b). The electrostatic interaction and the flexible histidine sidechains allow some wobble in the binding site leading to the symmetric arrangement observed in the crystal structure.

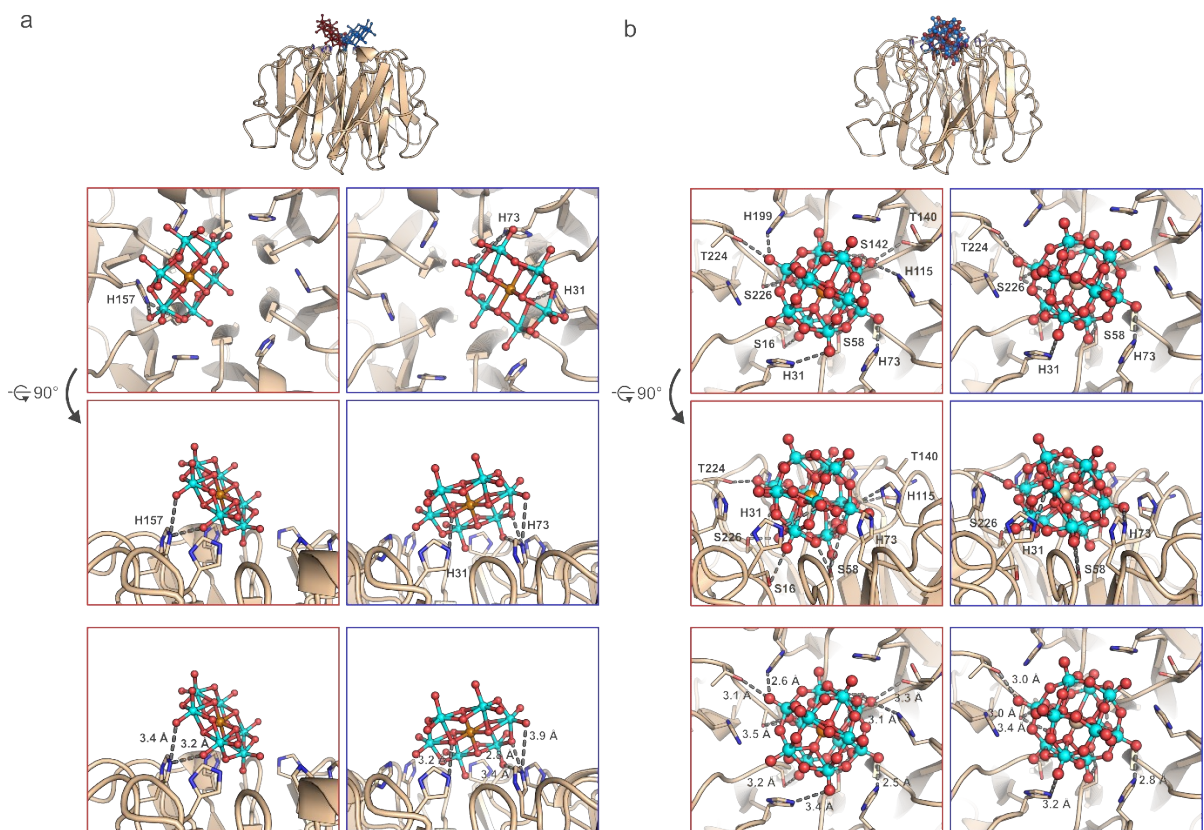


Figure S9. Alternate orientations of the POMs in the Pizza6 + TEW (a) and Pizza6 + STA ($P2_1$) (b) crystals.

The binding of POMs to Pizza6-S at pH 6 and higher buffered conditions revealed unordered binding. a) The interactions of two alternate positions of TEW to the pocket of Pizza6-S, b) two orientations of STA and their respective interactions with the protein ($P2_1$).

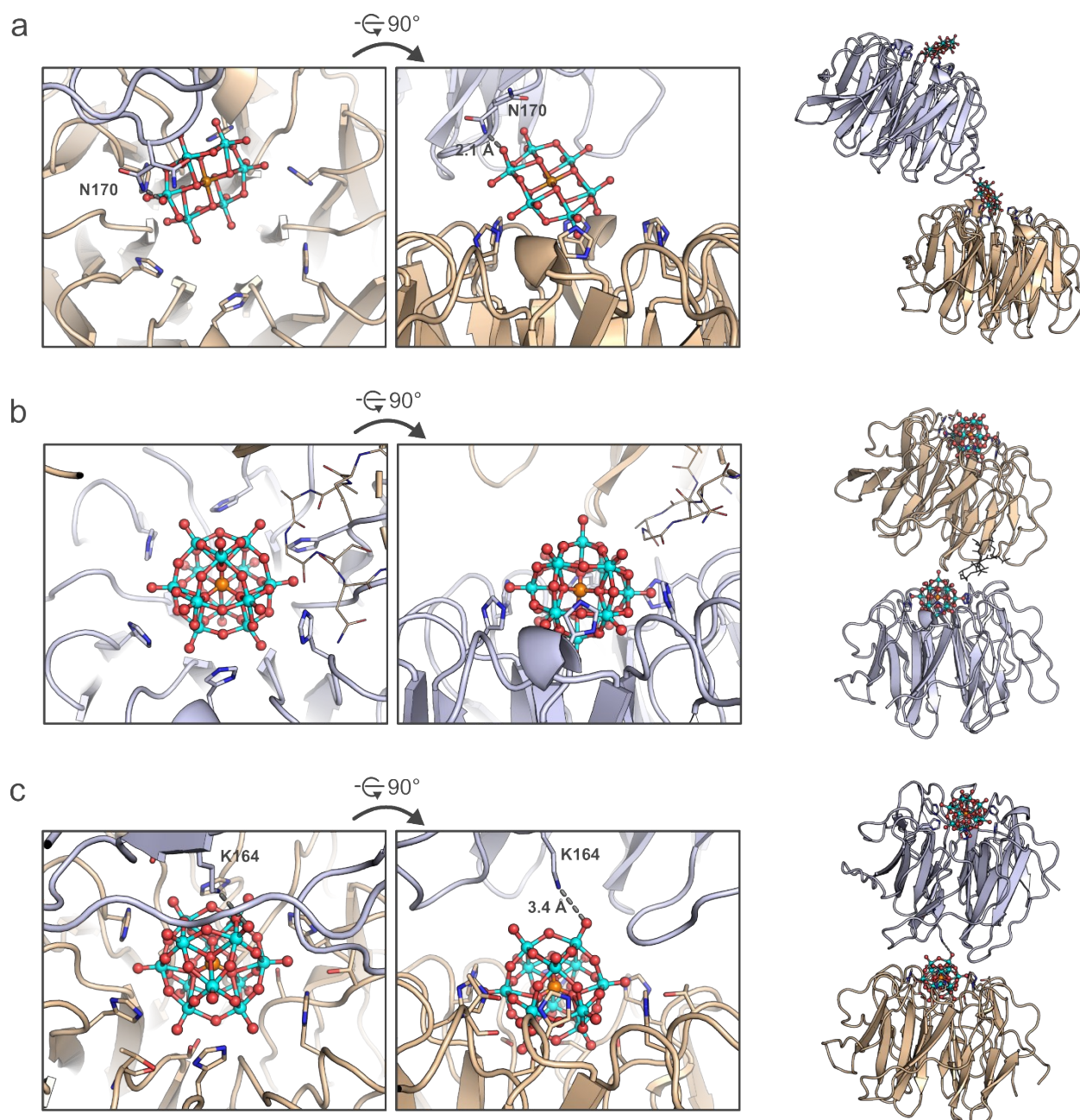


Figure S10. The Keggin and Anderson-Evans type POMs binding mode is not influenced by crystal packing contacts in the crystallisation buffer at pH 6 or above.

TEW only makes a single hydrogen bond with an asparagine from a neighboring Pizza6-S protein (a). For STA two different POMs are located in the asymmetric unit ($P2_1$). The first (b) only makes van der Waals interactions, while the second has a salt-bridge with a lysine (c).

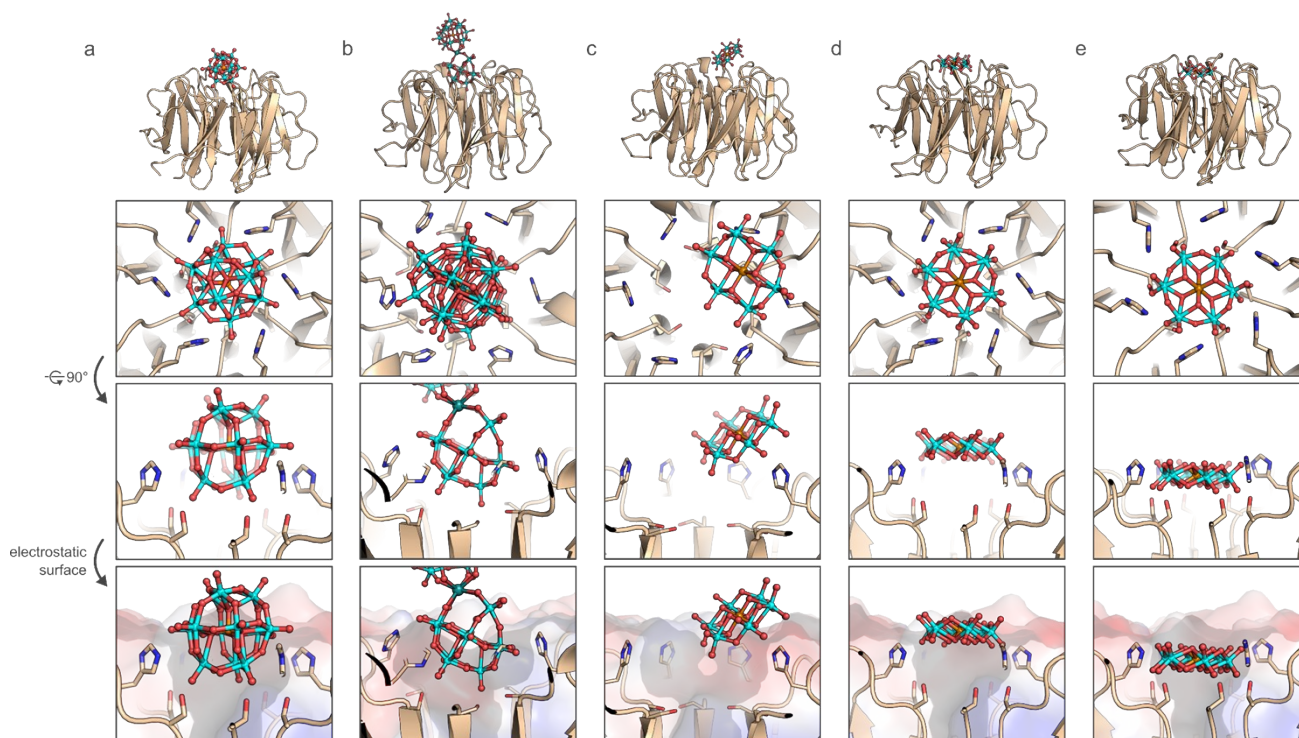


Figure S11. Complementarity and shape and hydrogen bonding determines specificity of the Pizza6S for Keggin type over Anderson-Evans type POMs.

Both the STA (a) and the Ce-K (b) fit the P6-S cavity well and satisfy all hydrogen bonds with the serines and histidines. In case of the TEW crystal structure it is clear the cavity is only partially matched (c). Attempts to fit the TEW according to the symmetry axis either satisfy the hydrogen bonds but leave the cavity mainly unoccupied (d) or exhibit a steric clash in an attempt to satisfy the serine hydrogen bonds (e).

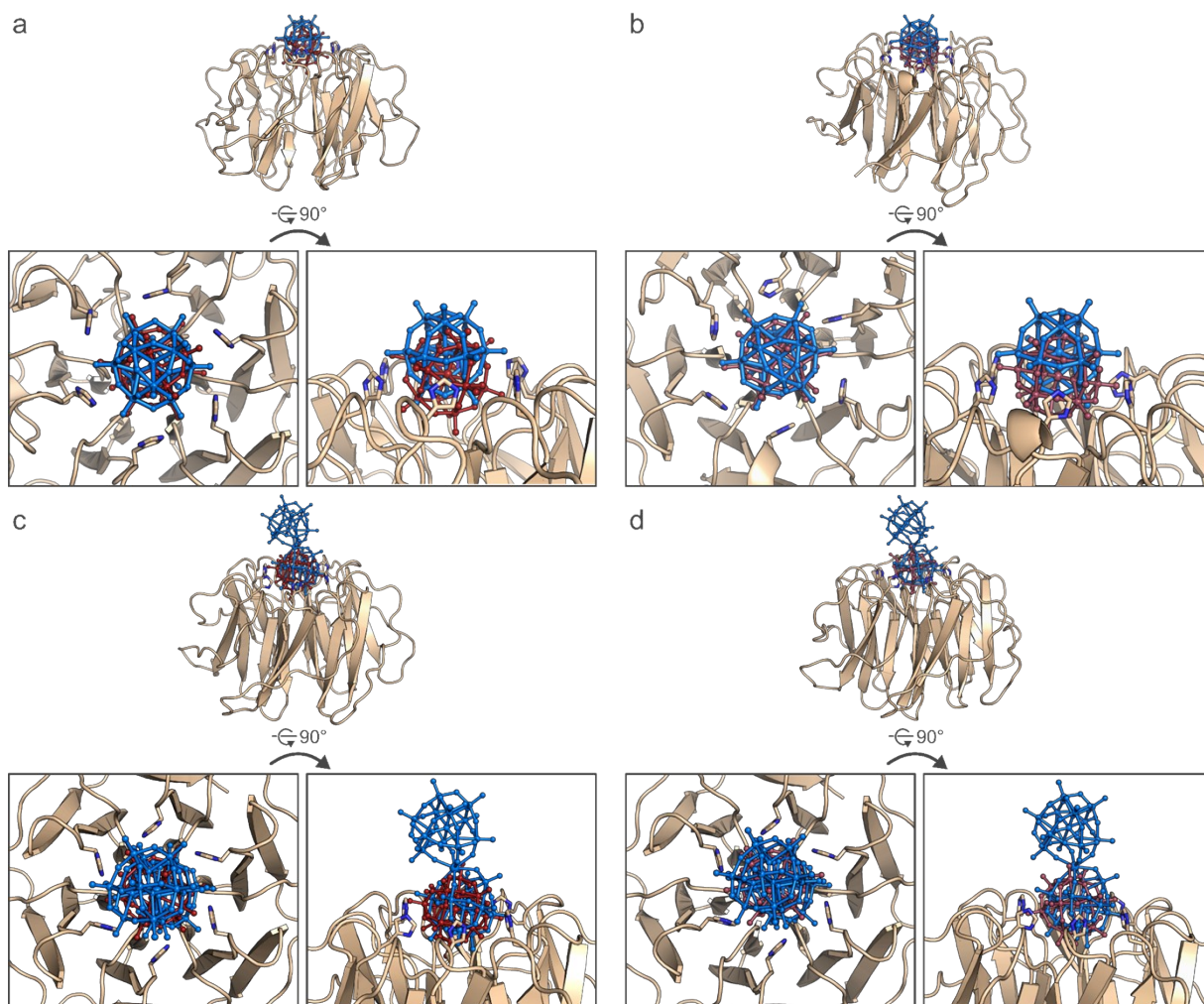


Figure S12. Comparison of STA binding under buffered conditions with STA and Ce-K under unbuffered conditions.

Both STA and Ce-K bind to the same surface of the protein, but the interactions are different at the atomic level. The POMs in the unbuffered crystal structures are shown in blue, while STA in the buffered crystal structure is shown in red.

Table S1. The effect of NaCl on binding affinity of Pizza6-S and POM at pH 6

Protein	POM	Concentration of NaCl (mM)	ITC	
			K_d (μ M) ^[a]	n ^[a]
Pizza6-S	STA	0	0.048 (0.034 - 0.065)	1.08 (1.07-1.09)
		100	0.036 (0.011 – 0.15)	0.96 (0.93-1.00)
		300	0.24 (0.14 – 0.41)	0.93 (0.90-0.95)

[a] Values in parentheses show the 68.3 % confidence interval.

Table S2. Overview of crystallisation conditions.

Protein	POMs	Crystal No.	Protein conc. (mg/ml) ^[a]	POM conc. (mM) ^[a]	Reservoir solution	Cryo protectant	Crystallization time
Pizza6-S	----	1	10	----	0.1M BICINE pH 9.0, 1.6M Ammonium Sulfate	30% Glycerol	1 week
	TEW	1	20	3.5	0.1M HEPES pH 7.0, 22%(w/v) PEG6000	25% Glycerol	1 week
	STA ^[b]	1	20	3.5	1.5M Sodium malonate pH 6.0	20% Glycerol	1 week
		2	20	3.5	0.2M Potassium iodine, 20% (w/v) PEG3350	30% Glycerol	1 week
	Ce-K	1	20	3.5	0.05M Magnesium acetate, 0.1M Sodium acetate, 10% (w/v) PEG8000	30% Glycerol	1 week

[a] The concentrations shown are stock solutions. The final concentrations in the drop are 5 mg/mL protein and 0.875 mM POM. [b] crystals 1 and 2 are space group $P2_1$ and $C2$, respectively.

Table S3. Crystallographic data collection and refinement statistics.

	Apo Pizza6-S		Pizza6-S with				Ce-K
			TEW		STA		
			$P2_1$	$C2$			
PDB code	6QSD	6QSE		6QSF	6QSG		6QSH
Data collection							
Diffraction source	SOLEIL, Proxima-1	DLS, I-04		DLS, I-04	DLS, I-04		DLS, I-04
Wavelength (Å)	0.97857	0.9795		0.9795	0.9795		1.8500
Resolution range (Å)	43.91-1.45 (1.47-1.45)	43.84-1.90 (1.94-1.90)		47.64-1.50 (1.53-1.50)	37.82-1.15 (1.17-1.15)		48.39-2.50 (2.60-2.50)
Space group	$P2_12_12_1$	$P2_12_12_1$		$P2_1$	$C2$		$P22_12_1$
a, b, c (Å)	48.79, 56.42, 69.92	53.42, 56.47, 69.54			49.24, 69.78, 62.67	77.37, 44.67, 65.25	53.37, 67.26, 69.68
α, β, γ (°)	90.00, 90.00, 90.00	90.00, 90.00, 90.00			90.00, 104.67, 90.00	90.00, 113.28, 90.00	90.00, 90.00, 90.00
Reflections (measured/unique)	256,813/33,717	217,880/17,194		424,332/65,621	470,457/72,659		57,033/9,133
Completeness (%)	96.8 (95.0)	100.0 (100.0)		99.9 (99.5)	100.0 (99.8)		99.9 (100.0)
Mean I/ σ (I)	9.7 (2.1)	15.9 (3.5)		9.9 (2.3)	14.1 (3.5)		8.5 (3.3)
Multiplicity	7.6 (7.9)	12.7 (13.0)		6.5 (6.2)	6.5 (5.6)		6.2 (6.3)
$R_{\text{pim}}^{\text{[a]}}$	0.055 (0.320)	0.043 (0.397)		0.072 (0.575)	0.037 (0.279)		0.146 (0.523)
CC(1/2) ^[b]	0.996 (0.849)	0.998 (0.884)		0.996 (0.677)	0.998 (0.983)		0.993 (0.802)
Wilson B factor (Å ²)	14.2	22.6		16.6	6.2		6.0
Refinement statistics							
Resolution range (Å)	36.91-1.45	43.84-1.90		47.64-1.50	29.97-1.15		42.37-2.50
$R_{\text{work}}^{\text{[c]}}$	0.174	0.201		0.224	0.168		0.258
$R_{\text{free}}^{\text{[c]}}$	0.209	0.248		0.238	0.186		0.323
# of atoms							
Protein	1,837	1,786		3,654	1,814		1,749
Ligand	10	124		159	318		412
Water	239	121		233	198		21
R.m.s. deviations from ideal							
Bond lengths (Å)	0.013	0.020		0.012	0.008		0.003
Bond angles (°)	1.313	1.006		1.198	1.031		0.437

Chiral volumes (Å ³)	0.106	0.051	0.078	0.083	0.043
Ramachandran plot, residues in (%)					
Most favorable region	97.98	97.19	95.56	98.39	88.02
Allowed region	2.02	2.81	4.24	1.61	11.16
Average B factor (Å ²)					
Main chain (A)	19.0	22.7	19.1	17.6	32.3
Side chains (A)	21.57	28.99	21.41	21.70	28.78
Main chain (B)	/	/	22.12	/	/
Side chains (B)	/	/	24.20	/	/
POMs	/	53.40	19.27	25.73	29.75
Waters	33.174	29.49	27.41	29.08	18.83

[a] $R_{\text{pim}} = \frac{\sum_{\text{hkl}} [1/(N-1)]^{1/2} \sum_i |I_i(\text{hkl}) - \langle I(\text{hkl}) \rangle|}{\sum_{\text{hkl}} \sum_i I_i(\text{hkl})}$, where $I_i(\text{hkl})$ is the intensity of an observation, $\langle I(\text{hkl}) \rangle$ is the mean value for that reflection and the summations are over all reflections. [b] $\text{CC}(1/2) = \frac{\sum (x-\langle x \rangle)(y-\langle y \rangle)}{[\sum (x-\langle x \rangle)^2 \sum (y-\langle y \rangle)^2]^{1/2}}$. [c] R-factor = $\frac{\sum_{\text{hkl}} ||F_{\text{obs}}| - |F_{\text{calc}}||}{\sum_{\text{hkl}} |F_{\text{obs}}|}$, where F_{obs} and F_{calc} are the observed and calculated structure-factor amplitudes, respectively. The free R-factor was calculated with 5% of the data excluded from the refinement. Values in brackets are for the outer shell.

Table S4. The occupancies of TEW, STA and Ce-K in their respective co-crystals.

	Occupancy			
	Pizza6-S - TEW	Pizza6-S - STA (C2)	Pizza6-S - STA (P2 ₁)	Pizza6-S - Ce-K
Position 1 ^[a]	100%	50% ^[b]	97%	50% ^[b]
Orientation A	25%	25% ^[b]	/	23% ^[b]
Orientation B	24%	25% ^[b]	/	14% ^[b]
Orientation C	24%	/	/	13% ^[b]
Orientation D	27%	/	/	/
Position 2 ^[a]	/	19%	92%	100%
Orientation A	/	6%	31%	/
Orientation B	/	3%	61%	/
Orientation C	/	5%	/	/
Orientation D	/	5%	/	/

[a] Each position might consist of multiple alternative orientations. The occupancy given is the total of the sum of the occupancy of each individual orientation at this position. [b] The molecule is located on a special position, meaning it is superposed with its symmetry equivalent molecule, resulting in a total occupancy in the crystal that is double that of the given value.

Table S5. Calculated volume and percentage of voids in the crystal packings

Crystal	Voids in the crystal packing	
	Percentage within unit cell	Volume (nm ³)
Pizza6-S	21.6%	41.4
Pizza6-S + TEW	25.8%	54.2
Pizza6-S + STA ($P2_1$)	25.9%	54.0
Pizza6-S + STA ($C2$)	24.5%	50.8
Pizza6-S + Ce-K	34.5%	86.4

References

1. Noguchi H, Mylemans B, De Zitter E, Van Meervelt L, Tame JRH, Voet A. *Biochem Biophys Res Commun.* 2018 Mar 18;497(4):1038–42.
2. Voet ARD, Noguchi H, Addy C, Simoncini D, Terada D, Unzai S, et al. *Proc Natl Acad Sci U S A.* 2014 Oct 21;111(42):15102–7.
3. Scroggie AG, Clark GL. *Proc Natl Acad Sci.* 1929 Jan 15;15(1):1–8.
4. Ilyas Z, Shah HS, Al-Oweini R, Kortz U, Iqbal J. *Metallomics.* 2014;6(8):1521–6.
5. Griffith WP, Morley-Smith N, Nogueira HIS, Shoair AGF, Suriaatmaja M, White AJP, et al. *J Organomet Chem.* 2000 Aug 11;607(1–2):146–55.
6. Goovaerts V, Stroobants K, Absillis G, Parac-Vogt TN. *J Inorg Biochem.* 2015;150:72–80.
7. Keller S, Vargas C, Zhao H, Piszczek G, Brautigam CA, Schuck P. *Anal Chem.* 2012 Jun 5;84(11):5066–73.
8. Brautigam CA, Zhao H, Vargas C, Keller S, Schuck P. *Nat Protoc.* 2016 May 1;11(5):882–94.
9. Scheuermann TH, Brautigam CA. *Methods.* 2015 Apr 1;76:87–98.
10. Zhao H, Piszczek G, Schuck P. *Methods.* 2015 Apr 1;76:137–48.
11. Brautigam CA. Academic Press Inc.; 2015. p. 109–33.
12. Schuck P, Perugini MA, Gonzales NR, Hewlett GJ, Schubert D. *Biophys J.* 2002;82(2):1096–111.
13. Lebowitz J, Lewis MS, Schuck P. Modern analytical ultracentrifugation in protein science: A tutorial review. *Protein Sci.* 2009 Jan 1;11(9):2067–79.
14. Kabsch W. XDS. *Acta Crystallogr Sect D Biol Crystallogr.* 2010;66(2):125–32.
15. Kabsch W. *Acta Crystallogr Sect D Biol Crystallogr.* 2010;66(2):133–44.
16. Evans PR, Murshudov GN. *Acta Crystallogr Sect D Biol Crystallogr.* 2013;69(7):1204–14.
17. McCoy AJ, Grosse-Kunstleve RW, Adams PD, Winn MD, Storoni LC, Read RJ. *J Appl Crystallogr.* 2007;40(4):658–74.
18. Afonine P V, Grosse-Kunstleve RW, Echols N, Headd JJ, Moriarty NW, Mustyakimov M, et al. *Acta Crystallogr D.* 2012;68(4):352–67.
19. Adams PD, Afonine P V, Bunkóczi G, Chen VB, Davis IW, Echols N, et al. *Acta Crystallogr Sect D Biol Crystallogr.* 2010;66(2):213–21.
20. Emsley P, Lohkamp B, Scott WG, Cowtan K. *Acta Crystallogr Sect D Biol Crystallogr.* 2010;66(4):486–501.
21. Chen VB, Arendall WB, Headd JJ, Keedy DA, Immormino RM, Kapral GJ, et al. *Acta Crystallogr Sect D Biol Crystallogr.* 2010;66(1):12–21.
22. DeLano WL. The PyMOL Molecular Graphics System. Schrödinger LLC www.pymol.org [Internet]. 2002;Version 1.:<http://www.pymol.org>-<http://www.pymol.org>. Available from: <http://www.pymol.org>
23. Touw WG, Baakman C, Black J, Te Beek TAH, Krieger E, Joosten RP, et al. *Nucleic Acids Res.* 2015 Jan 28;43(D1):D364–8.
24. Kabsch W, Sander C. *Biopolymers.* 1983;22(12):2577–637.
25. Jurrus E, Engel D, Star K, Monson K, Brandi J, Felberg LE, et al. *Protein Sci.* 2018 Jan 1;27(1):112–28.
26. Macrae CF, Bruno IJ, Chisholm J a., Edgington PR, McCabe P, Pidcock E, et al. *J Appl Crystallogr.* 2008;41(2):466–70.
27. Moriarty NW, Grosse-Kunstleve RW, Adams PD. *Acta Crystallogr Sect D Biol Crystallogr.* 2009;65(10):1074–80.

28. Tsuboi M, Uchida S. Private communication to Cambridge Structural Database, refcode = AZEPUS. 2016.
29. Iijima J, Ishikawa E, Nakamura Y, Naruke H. *Inorganica Chim Acta*. 2010;363(7):1500–6.
30. Vagin AA, Steiner RA, Lebedev AA, Potterton L, McNicholas S, Long F, et al. *Acta Crystallogr Sect D Biol Crystallogr*. 2004 Dec 1;60(12):2184–95.

Author Contributions

Polyoxometalates used in this work were synthesized and characterized by Drs. Laurens Vandebroek. Protein expression and purification was performed by Dr. Hiroki Noguchi. Crystallization, x-ray diffraction, data processing and structural modeling were performed by Drs. Laurens Vandebroek and Dr. Hiroki Noguchi. Drs. Kenichi Kamata and Dr. Hiroki Noguchi performed ITC and AUC experiments under the supervision of Prof. Jeremy R.H. Tame. Validation of the final structural models was performed by Prof. Luc Van Meervelt. Prof. Tatjana N. Parac-Vogt provided valuable insights into the interpretation and consolidation of all results reported in this publication Prof. Arnout R.D. Voet supervised the analysis of the supramolecular frameworks and provided insight into the design of the symmetrical proteins.